



**POLITECNICO
MILANO 1863**

Department of Aerospace Science and Technology

**6U Cubesat
Detumbling, Slew Manoeuvre and Sun Pointing
Spacecraft Attitude Dynamics And Control
Final Project**





Contents

| | | |
|----------|--|-----------|
| 1 | Introduction | 1 |
| 2 | List of Parameters | 2 |
| 2.1 | Legend: | 2 |
| 2.2 | List of selected data for the Simulink simulation: | 2 |
| 3 | Structure | 4 |
| 4 | ADCS architecture : | 4 |
| 4.1 | On board instrumentation: | 4 |
| 4.1.1 | gyro: | 4 |
| 4.1.2 | magnetometer: | 5 |
| 4.2 | Actuators: | 5 |
| 4.2.1 | Magneto torquer: | 5 |
| 4.2.2 | Reaction wheels: | 6 |
| 4.2.3 | Cold-Gas Thrusters | 7 |
| 5 | Power,Mass and Volume Budget: | 7 |
| 6 | Model description | 8 |
| 6.1 | Assumptions and approximations: | 8 |
| 6.1.1 | Orbital mechanics: | 8 |
| 6.1.2 | Satellite dynamics and attitude: | 8 |
| 6.1.3 | Sun position: | 9 |
| 6.1.4 | Cold-Gas thruster: | 9 |
| 6.2 | Mathematical Model: | 10 |
| 6.2.1 | Reference frame: | 10 |
| 6.2.2 | Euler Equation: | 10 |
| 6.2.3 | Attitude: | 10 |
| 6.2.4 | Gravity Gradient torque: | 11 |
| 6.2.5 | SRP: | 11 |
| 6.2.6 | Magnetic disturbance: | 12 |
| 6.2.7 | Gyro | 13 |
| 6.2.8 | Magnetometer: | 14 |
| 6.2.9 | Magneto torquer: | 14 |
| 6.2.10 | Reaction wheels: | 15 |
| 6.2.11 | Cold-Gas thrusters | 15 |
| 7 | Control and determination Algorithms | 16 |
| 7.1 | De-tumbling | 16 |
| 7.1.1 | Kalman Filter: | 16 |
| 7.1.2 | Kalman Filter for DCM | 17 |
| 7.1.3 | Control law for the Magneto Torquer: | 17 |
| 7.1.4 | Bang Bang Control: | 18 |
| 7.2 | Slew Manoeuvre: | 18 |
| 7.2.1 | Sun Pointing: | 19 |
| 7.2.2 | Ideal Control: | 19 |
| 7.2.3 | Real Control: | 19 |
| 7.3 | Tracking | 19 |

| | |
|--------------------------------|-----------|
| 7.3.1 Pointing | 20 |
| 7.3.2 Ideal control: | 20 |
| 8 Results | 21 |
| 8.1 Detumbling | 21 |
| 8.2 Slew Manoeuvre | 22 |
| 8.3 Sun Pointing | 24 |
| 9 Conclusions | 25 |
| References | 26 |



1 Introduction

A CubeSat (U-class spacecraft) is a miniaturized satellite made for space purposes and is composed by multiples of $10 \times 10 \times 10$ cm cubic units. The mass is no more than 1.33 kilograms per unit, and often characterized by commercial off-the-shelf (COTS) components for their electronics and structure. CubeSats are commonly put in orbit by deployers on the International Space Station, or launched as secondary payloads on a launch vehicle. The intent is to provide affordable access to space for the university science community, Government agencies and commercial groups thanks to a standardized design of the whole structure. Uses typically involve experiments that can be miniaturized or serve purposes such as Earth observation [1]. Concerning the 6U (adopted in this project) is essentially the same as two 3Us side-by-side, making it twice as wide. Here listed there are the main features of the mission, deepened and developed through the project:

1. The satellite is set on a GEO orbit whose aim, after the de-tumbling phase, is to point the Sun.
2. The de-tumbling relies on a magnetometer and on a gyro for the attitude and dynamics determination. Subsequently for slew and pointing only the magnetometer is allowed to perform the reconstruction of the attitude matrix.
3. Since ,After several attempts with 1 magneto torquers, the Cubesat is not able to de-tumble in a reasonable time span,as an exception, 4 Cold-Gas thrusters are located at the base of the spacecraft itself. Regarding the control actuation ,for the last part of the mission, the system is fitted with 4 reaction wheels.

2 List of Parameters

2.1 Legend:

This is the convention adopted for representing scalar, vector and matrix quantities:

- (a) a = scalar representation (b) \mathbf{a} = vector representation (c) \mathbf{A} = matrix representation

2.2 List of selected data for the Simulink simulation:

| Variable | Description | Value | Unit of measure |
|-------------------------|--|--|---------------------|
| a_{geo} | initial semi major axis | 42164 | [km] |
| e_{geo} | initial eccentricity | 0 | [−] |
| i_{geo} | initial inclination | 0 | [rad] |
| ω_{geo} | initial anomaly of perigee | 0 | [rad] |
| Ω_{geo} | initial right ascension of the ascending node | 0 | [rad] |
| θ_{geo} | initial true anomaly | 0 | [rad] |
| $\boldsymbol{\omega}_1$ | initial angular velocity vector for detumbling | [0.22 0.26 0.22] | [rad/s] |
| $\boldsymbol{\omega}_2$ | initial angular velocity vector for Slew | $10^{-4} [4.31 \quad 3.31 \quad -3.08]$ | [rad/s] |
| $\boldsymbol{\omega}_3$ | initial angular velocity vector for Pointing | $10^{-5} [-0.36 \quad 0.34 \quad -0.66]$ | [rad/s] |
| \mathbf{A}_1 | initial attitude matrix for de-tumbling | $\begin{bmatrix} 0.5335 & 0.808 & 0.25 \\ -0.808 & 0.3995 & 0.433 \\ 0.25 & -0.433 & 0.866 \end{bmatrix}$ | [−] |
| \mathbf{A}_2 | initial attitude matrix for Slew | $\begin{bmatrix} 0.4777 & -0.0636 & 0.8762 \\ -0.7262 & 0.5327 & 0.4345 \\ -0.4944 & -0.8439 & 0.2083 \end{bmatrix}$ | [−] |
| \mathbf{A}_3 | initial attitude matrix for Pointing | $\begin{bmatrix} 0.8660 & 0.4589 & 0.1989 \\ -0.4996 & 0.7757 & 0.3856 \\ 0.0226 & -0.4333 & 0.9009 \end{bmatrix}$ | [−] |
| $T_{detumbling}$ | integration time of detumbling | 180 | [s] |
| T_{slew} | integration time of slew | 140 | [s] |
| $T_{pointing}$ | integration time of pointing | 86400 | [s] |
| M | mass of the Cubesat | 12 | [Kg] |
| w | width of the Cubesat | 226.3 | [mm] |
| l | length of the Cubesat | 100 | [mm] |
| a | height of the Cubesat | 366 | [mm] |
| \mathbf{I} | Inertia matrix | $\begin{bmatrix} 0.218 & 0 & 0 \\ 0 & 0.166 & 0 \\ 0 & 0 & 0.082 \end{bmatrix}$ | [Kgm ²] |
| f_g | Gyro frequency | 262 | [Hz] |



| Variable | Description | Value | Unit of measure |
|---------------------------|--|--|---------------------|
| σ_n | Gyro Noise | 0.15 | [°/ \sqrt{h}] |
| σ_b | Gyro Bias | 0.3 | [°/h] |
| σ_w^2 | diagonal term of \mathbf{R} | 10^{-8} | [rad 2 /s 4] |
| σ_v^2 | diagonal term of \mathbf{Q} | 10^{-8} | [rad 2 /s 2] |
| f_m | Magnetometer frequency | 18 | [Hz] |
| p_{acc} | Magnetometer pointing acc. | 30 | [arcmin] |
| m_{mt} | Magnetic moment of the magneto torquer | 1.2 | [Am 2] |
| \mathbf{m}_{SC} | parasitic magnetic moment | [0.1 0.1 0.1] | [Am 2] |
| m_{max} | maximum torque of a RW | 1 | [mNm] |
| \mathbf{A} | matrix disposition of the reaction wheels | $\begin{bmatrix} 1 & 0 & 0 & \frac{1}{\sqrt{3}} \\ 0 & 1 & 0 & \frac{1}{\sqrt{3}} \\ 0 & 0 & 1 & \frac{1}{\sqrt{3}} \end{bmatrix}$ | [-] |
| \mathbf{A}^* | pseudo inverse of \mathbf{A} | $\begin{bmatrix} \frac{5}{6} & -\frac{1}{6} & -\frac{1}{6} \\ -\frac{1}{6} & \frac{5}{6} & -\frac{1}{6} \\ -\frac{1}{6} & -\frac{1}{6} & \frac{5}{6} \\ \frac{1}{2\sqrt{3}} & \frac{1}{2\sqrt{3}} & \frac{1}{2\sqrt{3}} \end{bmatrix}$ | [-] |
| RL_{RW} | rate limiter of a RW | 10 | [mNm/s] |
| m_{max} | max transmitted torque | 1 | [mNm] |
| M_{st} | max momentum storage for RW | 10 | [mNms] |
| F | Thrust of a Cold-Gas thruster | 10 | [mN] |
| $\tau_{Cold-Gas_{rise}}$ | rise time for the Cold-Gas thruster | 10 | [ms] |
| $\tau_{Cold-Gas_{fall}}$ | fall time for the Cold-Gas thruster | 50 | [ms] |
| $\tau_{Cold-Gas_{delay}}$ | delay time for the Cold-Gas thruster | 5 | [ms] |
| $\epsilon_{Cold-Gas}$ | minimum value of ω to avoid chattering | $5 \cdot 10^{-4}$ | [rad/s] |
| \mathbf{C} | sensor matrix of the Kalman filter | $\begin{bmatrix} 1 & 0 & 0 \\ 0 & 1 & 0 \\ 0 & 0 & 1 \end{bmatrix}$ | [-] |
| k_{DCM} | tuning parameter for the DCM filter | 0.1 | [-] |
| k_1 | prop.coeff of ω_e for the ideal control | 0.15 | [Nm/rad] |
| k_2 | prop.coeff related to \mathbf{A}_e for the ideal control | 0.005 | [Nm] |
| r_{sun} | distance Earth-Sun | 149600000 | [km] |
| B | Initial phase of the Sun | $\frac{\pi}{6}$ | [rad] |



3 Structure

The physical dimensions of the spacecraft are depicted by the following image 1:

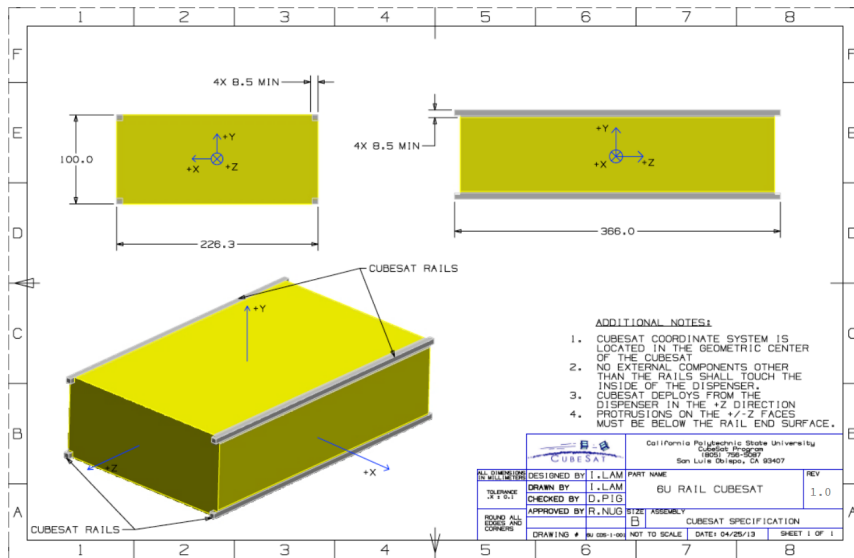


Figure 1: 6U Cubesat dimensions specification [2]



Figure 2: 6-Unit cubesat structure [4]

The ISIS 6-Unit CubeSat 2 structure is developed as a modular satellite structure based upon the CubeSat standard. The design created by ISIS allows for multiple configurations, giving CubeSat developers maximum flexibility in their design process. The hardware can be mounted directly inside with stacks or on the frame itself. Every device on board is accessible before mounting external hardware surfaces. Here the main features are shown [4]:

- cost: €7350
- Outside Envelope ($l \times w \times h$) $100 \times 226.3 \times 366 \text{ mm}$
- Primary + Secondary Structure Mass 1.1 kg
- Inside Envelope ($l \times w \times h$) per module ($6 \times$) $96 \times 96 \times 89.4 \text{ mm}$
- Thermal Range (min – max) -40 to +80 °C

4 ADCS architecture :

4.1 On board instrumentation:

4.1.1 gyro:



Figure 3: STIM300 [3]

The gyro works during the de-tumbling part for the dynamic determination. It measures the angular velocity of the satellite. STIM300 is a small, tactical grade, low weight, high performance non-GPS aided Inertial Measurement Unit (IMU). It contains 3 highly accurate MEMS gyros, 3 high stability accelerometers and 3 inclinometers. The IMU is factory calibrated and compensated over its entire operating temperature range.



- cost: € n.d
- Update rate: 262Hz
- Bias: < 0.3°/ h
- Noise: < 0.15°/√h
- Volume: 35 cm³
- Mass: 0.55kg
- nominal Power: 1.5 W
- Thermal (operational): -40 °C to +85 °C
- Insensitive to magnetic fields

4.1.2 magnetometer:



Figure 4: NSS Magnetometer [5]

The sensor provides x, y and z-axes magnetic field component measurements, in the body reference frame. Mounted outside the spacecraft at the end of a rigid boom the NewSpace Systems magnetometer includes low noise, precision processing and analogue-to-digital conversion circuitry. By knowing the local magnetic field of the Earth it is capable of measuring the attitude kinematics of the spacecraft. Furthermore it is useful for the calculation of magnetorquer rods control torque levels.

- cost: €14790
- Measurement range: -60,000 nT to +60,000 nT
- Update rate: < 18Hz
- Resolution: < 8 nT
- Pointing accuracy: 0.5 °
- Dimensions: 96 × 43 × 17mm
- Mass: < 85g
- Power: < 750mW
- Thermal (operational): -25°C to +70 °C
- Power supply: +5V DC

4.2 Actuators:

4.2.1 Magneto torquer:



Figure 5: NCTR-M012 Magnetotorquer Rod [6]

Magnetorquers offer a way of controlling the attitude of a satellite. This can be attained by means of the interaction of the local Earth's magnetic field.

Operating a magnetic alloy rod produces an amplification effect over an air cored magnetotorquer. This requires less power, which is critical for CubeSat missions. The rods can enable a mission with increased manoeuvrability and reduced detumble rates.

CubeSat Magnetotorquer rods are designed to be run directly from a switched 5 Volt power output from the on-board power control system.

In the assigned project only 1 Magnetotorquer is provided with these properties [6]:



- cost: €1750
- Magnetic moment: 1.2 Am^2
- Residual moment: $< 0.002 \text{ Am}^2$
- Operating range: -10 °C to +50 °C
- Power: 5 Volt
- Lifetime: > 10 years
- Dimensions: 94mm x 15 mm x 13 mm
- Mass: < 50 g

This particular rod 5 has some benefits to take into account . First things first it is a low cost standard product, it guarantees high moment for low power and is featured by small size and low mass , crucial for nano-satellites. In addition it has no residual moment.

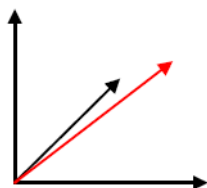
4.2.2 Reaction wheels:



Figure 6: CubeWheel Medium [7]

The CubeWheel Medium is a reaction wheel adopted to control the attitude of nanosatellites. The module contains a brushless DC motor with vacuum-rated bearings, as well as the required drive electronics and speed control algorithms. Specs:

- cost: €5,400
- Max torque: 1.0 mNm
- Average power consumption: <180 mW (@2000 RPM, 8V)
- momentum storage : 10 mNms
- Mass: 130 g
- Operating voltage: 3.3V / battery voltage (6.5V to 16V)
- Dimensions: 46 x 46 x 31.5 mm
- mountable in 3 axis



To work properly , during the slew and pointing phase of the mission , the reaction wheels should be at least 3 mounted on the axes. In case of redundancy a fourth momentum wheel could be added with the following layout 7. Whenever one of the 3 rotors fails the fourth still guarantees controllability.

Figure 7: Reaction wheels layout [8]

4.2.3 Cold-Gas Thrusters

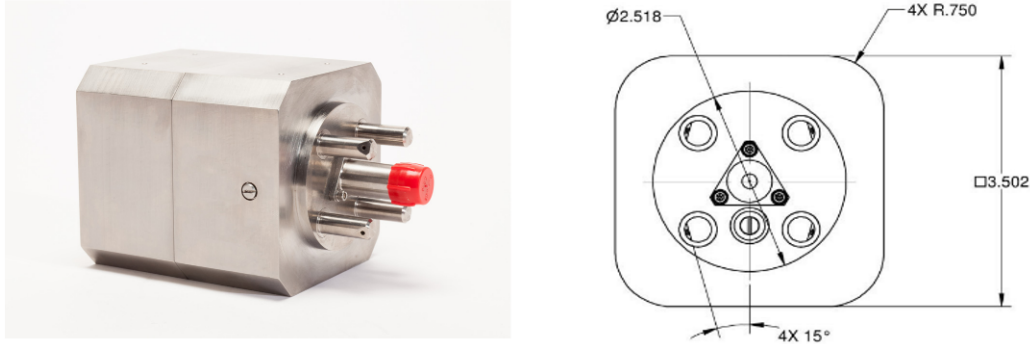


Figure 8: CubeWheel Medium [9]

The VACCO CubeSat Hybrid ADN Reaction Control System is a high performance micro propulsion system (MiPS) specifically designed for CubeSats. The smart feed system automatically provides closed-loop thrust vector control during delta-v burns. Reliability is ensured through simplicity of design, welded titanium construction and frictionless valve technology.

- cost: nd
- MIB 0.1 mN-s
- Smart, self-contained propulsion system
- Mass 1.797 kg
- One 100 mN ECAPS ADN thruster
- Power: < 15 [W] during hot-fire,< 0.055 [W] in standby mode
- Four 10 mN cold gas ACS thruster
- $I_s p = 60\text{s}$

5 Power,Mass and Volume Budget:

| Components | sources | # | Mass [kg] | Tot.Mass [kg] | Power [W] | Tot.Power | V [cm^3] | Tot.V [cm^3] |
|--------------------------|---------|---|-----------|---------------|-----------|--------------|-----------|---------------|
| Structure | EU | 1 | 1.1 | 1.1 | X | X | 8283 | 8283 |
| Gyro | EU | 1 | 0.1 | 0.1 | 1 | 1 | 131 | 131 |
| Magnetometer | EU | 1 | 0.085 | 0.085 | 0.75 | 0.75 | 70 | 70 |
| RW | EU | 4 | 0.13 | 0.52 | 0.180 | 0.54 | 66 | 264 |
| Magneto torquer | EU | 1 | 0.05 | 0.05 | 0.2 | 0.2 | 21 | 21 |
| CG Thrusters | EU | 4 | 1.797 | 1.797 | 15 | 15 | 51.45 | 51.45 |
| TOTAL | | | | 2.552 | | 17.49 | | 537.45 |
| TOTAL margin(10%) | | | | 2,8072 | | 19,49 | | 591.20 |

Figure 9: Budget

Please notice that in the mass,volume and power budget additional on board devices are not taken into consideration such as: antennas,batteries,solar panels,.... and you name it. From the data available the evaluation of the inertia matrix referred to the principal axis is straightforward:

$$\mathbf{I} = \begin{bmatrix} 0.218 & 0 & 0 \\ 0 & 0.166 & 0 \\ 0 & 0 & 0.082 \end{bmatrix} [\text{kg}\text{m}^2] \quad (1)$$

6 Model description

6.1 Assumptions and approximations:

6.1.1 Orbital mechanics:

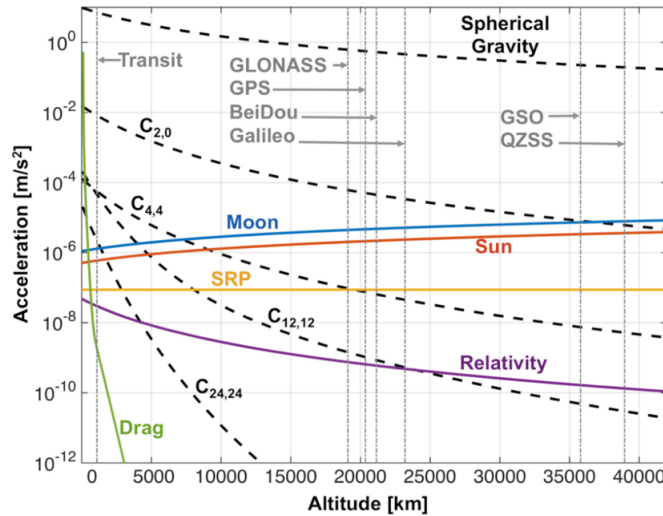


Figure 10: importance of orbital perturbations [10]

The satellite under analysis is set on a GEO orbit. For the the orbital mechanics , as to ease the solution process, the motion is modeled without any kind of perturbation due to : J2,SRP,Magnetic disturbance and so on and so forth. This is certainly a coarse approximation, since in reality the orbit is sensitive to all of them. On the other hand there is no presence of air in GEO orbit, so drag forces can be completely discarded. This picture summarizes the all effects said before:

6.1.2 Satellite dynamics and attitude:

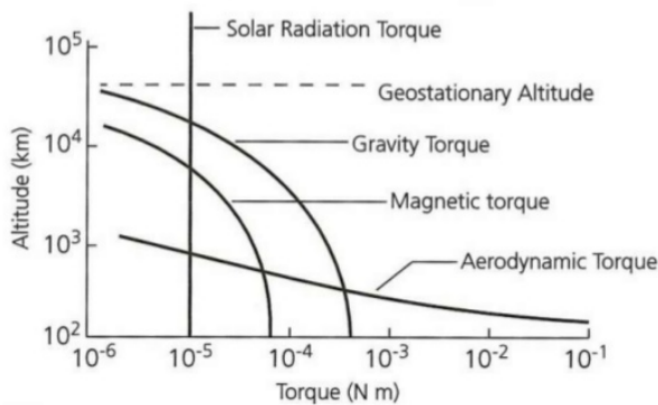
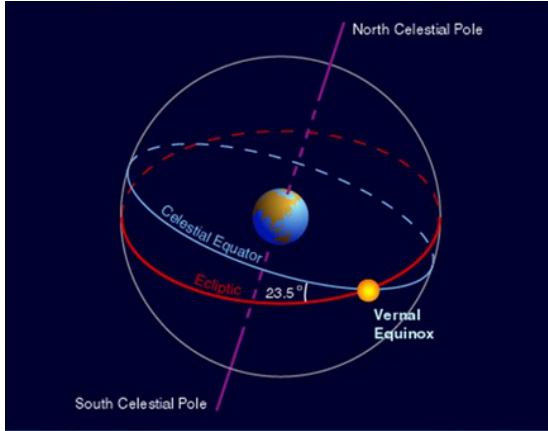


Figure 11: disturbance torques [11]

The aim is to study the local dynamics and to develop for this one control algorithms . In addition, aside from the de-tumbling which occurs in a small time frame, for slew and Sun pointing the perturbations

quoted before are all developed with different models in the following section. It is worth noting that the spacecraft is treated as rigid body, (*no vibrations or continuous mechanics involved*).

6.1.3 Sun position:



$$r_{Sun} = 149600000 \text{ [Km]} \quad (2)$$

$$\omega_{Sun} = \frac{2\pi}{365.25 \cdot 24 \cdot 3600} = 1.99 \cdot 10^{-7} \left[\frac{\text{rad}}{\text{s}} \right] \quad (3)$$

Figure 12: Sun position [12]

Since the inertial reference frame is located in the Earth equatorial reference frame, the position of the Sun will change over time , instead the earth will remain fixed. As first approximation the orbit described by the star is circular with constant angular velocity. Actually this is a good model because the eccentricity the Earth orbit is $e = 0.0167$, defining a nearly circular orbit.

6.1.4 Cold-Gas thruster:

Here the main assumption is that the satellite has a constant mass through the detumbling , when the Cold-Gas thruster operates.A rough approximation the mass flow rate is given by:

$$\dot{m}_p = \frac{2F}{Isp g_E} = 3.4 \cdot 10^{-5} \frac{Kg}{s} \quad (4)$$

Considering a detumbling time of 90s, the total expelled mass is :

$$m_{expelled} = 90 \cdot 3.4 \cdot 10^{-5} = 3 \cdot 10^{-3} \text{ Kg.} \quad (5)$$

6.2 Mathematical Model:

6.2.1 Reference frame:

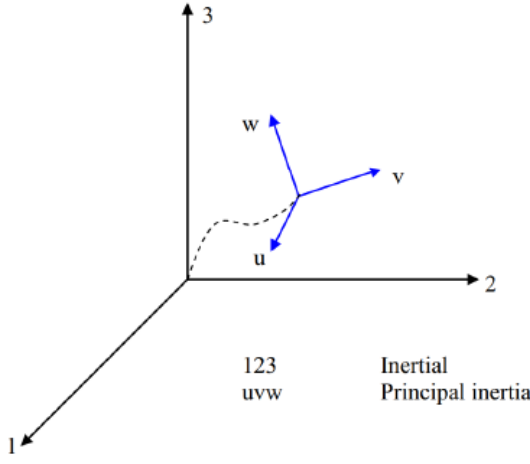


Figure 13: Inertial and body reference frame [13]

The transformation does not affect both the magnitude and the relative orientation of the unit vectors. These constraints are expressed by the following properties :

$$\mathbf{A}\mathbf{A}^T = \mathbf{I} \quad \text{and} \quad \det(\mathbf{A}) = 1 \quad (8)$$

In particular the inertial reference frame (*represented by the Earth itself*) and the body one are identified by :

$$\mathbf{N} = \begin{bmatrix} 1 & 0 & 0 \\ 0 & 1 & 0 \\ 0 & 0 & 1 \end{bmatrix} \quad (9) \qquad \mathbf{B} = \mathbf{A}_{\mathbf{B}/\mathbf{N}} \mathbf{N} \quad (10)$$

The matrix $\mathbf{A}_{\mathbf{B}/\mathbf{N}}$ will be evaluated at each time step , based on the relative orientation of the spacecraft with respect to the Earth.

6.2.2 Euler Equation:

The system of differential equations outlining the dynamics of the satellite, are the so called Euler equations:

$$\begin{cases} \dot{\omega}_x = \frac{I_y - I_z}{I_x} \omega_y \omega_z + \frac{M_x}{I_x} \\ \dot{\omega}_y = \frac{I_z - I_x}{I_y} \omega_z \omega_x + \frac{M_y}{I_y} \\ \dot{\omega}_z = \frac{I_x - I_y}{I_z} \omega_x \omega_y + \frac{M_z}{I_z} \end{cases} \quad (11)$$

Please notice that M_x, M_y and M_z comprises both the disturbances and the control actuation.

6.2.3 Attitude:

The ideal attitude matrix is governed by this system of differential equations:

$$\dot{\mathbf{A}}_{\mathbf{B}/\mathbf{N}} = -[\boldsymbol{\omega}^\wedge] \mathbf{A}_{\mathbf{B}/\mathbf{N}} \quad (12)$$

Despite this relation an instrument on board for detecting the attitude matrix is always needed. The attitude matrix along with the integration loses the orthonormal properties . There is an iterative procedure to retrieve these features :

$$\mathbf{A}_{k+1} = \frac{3}{2} \mathbf{A}_k - \mathbf{A}_k \mathbf{A}_k^T \mathbf{A}_k \frac{1}{2} \quad (13)$$

6.2.4 Gravity Gradient torque:

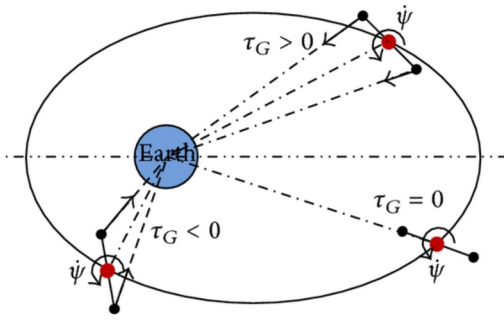


Figure 14: Gravity Gradient Torque [14]

The gravity field is not uniform, thus a torque could act on the satellite. This kind of perturbation is relevant for large satellites due to long time action. In its more generic definition the torque yielded by the elementary force f acting on the infinitesimal mass m is:

$$\mathbf{m}_{GG} = - \int_b \mathbf{r} \times \frac{Gm_E}{|r + r_{sc}|^3} (\mathbf{r}_{sc} + \mathbf{r}) dm \quad (14)$$

Where \mathbf{r}_{sc} is the position vector of the center of mass and r the one from the center of mass to any other point of the spacecraft.

$$r_{sc} \gg r \quad (15)$$

By making few steps (*here not reported*) and evaluating all the terms under the integral sign, the 14 turns into:

$$\mathbf{m}_{GG} = \frac{Gm_E}{r_{sc}^3} \begin{bmatrix} (I_z - I_y)c_2c_3 \\ (I_x - I_z)c_1c_3 \\ (I_y - I_x)c_1c_2 \end{bmatrix} \quad (16)$$

c_1, c_2 and c_3 are the direction cosines of the radial direction in principal axes.

6.2.5 SRP:

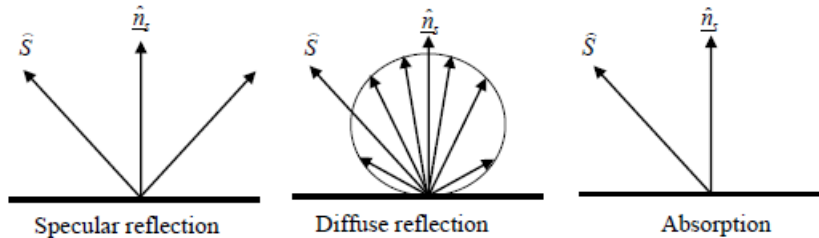


Figure 15: reflection and absorption [15]

Solar radiation, illuminating the surface of a satellite, determines the presence of a pressure, leading to a torque around the center of mass of the satellite. The are 2 sources of this kind of phenomena : the Sun and the Earth. The former has usually a stronger effect and it can be stated to be constant around our planet. The latter instead, resulted by reflection of the Sunlight is strongly dependent on the distance. The following table summarizes the typical values:



| Altitude (Km) | Direct solar radiation (W/m ²) | Radiation reflected by the Earth (W/m ²) | Earth radiation (W/m ²) |
|---------------|--|--|-------------------------------------|
| 500 | 1358 | 600 | 150 |
| 1000 | 1358 | 500 | 117 |
| 2000 | 1358 | 300 | 89 |
| 4000 | 1358 | 180 | 62 |
| 8000 | 1358 | 75 | 38 |
| 15000 | 1358 | 30 | 14 |
| 30000 | 1358 | 12 | 3 |
| 60000 | 1358 | 7 | 2 |

Figure 16: Typical values of SRP [15]

As a result the exchange of forces are as follows:

$$\mathbf{f} = PA(\hat{\mathbf{s}}_b \cdot \hat{\mathbf{n}}_s)[(1 - \rho_s)\hat{\mathbf{s}}_b + (2\rho_s(\hat{\mathbf{s}}_b \cdot \hat{\mathbf{n}}_s) + \frac{2}{3}\rho_d)\hat{\mathbf{n}}_s] \quad (18)$$

The knowledge or the attitude matrix $\mathbf{A}_{B/N}$ makes the calculation of the Sun position in the body frame easy:

$$\hat{\mathbf{s}}_b = \mathbf{A}_{B/N}\hat{\mathbf{s}}_N \quad (19)$$

The satellite is shaped like a cuboid, whose principal axes are oriented as the normal vectors of the outer surfaces:

$$\hat{\mathbf{n}}_{s1}^b = [1 \ 0 \ 0] \quad \hat{\mathbf{n}}_{s2}^b = [0 \ 1 \ 0] \quad \hat{\mathbf{n}}_{s3}^b = [0 \ 0 \ 1] \quad (20)$$

$$\hat{\mathbf{n}}_{s4}^b = [-1 \ 0 \ 0] \quad \hat{\mathbf{n}}_{s5}^b = [0 \ -1 \ 0] \quad \hat{\mathbf{n}}_{s6}^b = [0 \ 0 \ -1] \quad (21)$$

Last but not least the total torque acting on the satellite is now available:

$$\mathbf{t}_{SRP} = \begin{cases} \sum_{i=1}^{n_{surfaces}} \mathbf{c}_{pi} \times \mathbf{f}_i & if \ \hat{\mathbf{s}}_b \cdot \hat{\mathbf{n}}_{si}^b > 0 \\ 0 & if \ \hat{\mathbf{s}}_b \cdot \hat{\mathbf{n}}_{si}^b \leq 0 \end{cases} \quad (22)$$

6.2.6 Magnetic disturbance:

First of all before studying parasitic magnetic moment acting on the spacecraft, it is of paramount importance to derive the magnetic dipole model for the Earth. This approximation is suitable for space crafts orbiting with an altitude greater than 7000km but lower than 10 Earth radii. In the inertial frame the vector of the magnetic field \mathbf{b}_N is:

$$\mathbf{b}_N = \frac{R_E^3 H_0}{r^3} [3(\hat{\mathbf{m}}_E \cdot \hat{\mathbf{r}}_{sc})\hat{\mathbf{r}}_{sc} - \hat{\mathbf{m}}_E] \quad (23)$$

$$H_0 = \sqrt{(g_0^0)^2 + (g_1^1)^2 + (h_1^1)^2} \quad (24)$$

| | | IGRF 1995 | | IGRF 2000 | |
|---|---|-----------------------------|-----------------------------|-----------------------------|-----------------------------|
| n | m | g _n ^m | h _n ^m | g _n ^m | h _n ^m |
| 1 | 0 | -29682 | - | -29615 | - |
| 1 | 1 | -1789 | 5318 | -1728 | 5186 |

Figure 17: Gaussian coeff. in nT [16]

The versor along the dipole axis $\hat{\mathbf{m}}_E$ and the position one of the spacecraft $\hat{\mathbf{r}}_{sc}$ are:

$$\hat{\mathbf{m}}_E = [\sin(11.5^\circ)\cos(\omega_E t) \quad \sin(11.5^\circ)\sin(\omega_E t) \quad \cos(11.5^\circ)] \quad (25)$$

$$\hat{\mathbf{r}}_{sc} = [\cos(\omega_E t) \quad \sin(\omega_E t) \quad 0] \quad (26)$$

Then the magnetic field in the body frame \mathbf{b}_B is:

$$\mathbf{b}_B = \mathbf{A}_{B/N} \mathbf{b}_N \quad (27)$$

It can be measured by the magnetometer installed on board. The interaction between the local magnetic field ad the flow of current generates a torque given by the formula :

$$\mathbf{t}_{mag, dist} = \mathbf{m}_{sc} \times \mathbf{b}_B \quad (28)$$

\mathbf{m}_{sc} is the residual magnetic induction . The unit of measure of \mathbf{m}_{sc} can be stated as Am^2 . In order to simulate the presence of \mathbf{m}_{sc} it is reasonable to adopt an average constant value , which expresses a worst case scenario:

$$\mathbf{m}_{sc} = [0.1 \quad 0.1 \quad 0.1]^T [Am^2] \quad (29)$$

6.2.7 Gyro

The gyroscopes are implemented on board to measure the angular velocities. The components of this device can be depicted by the image shown below:

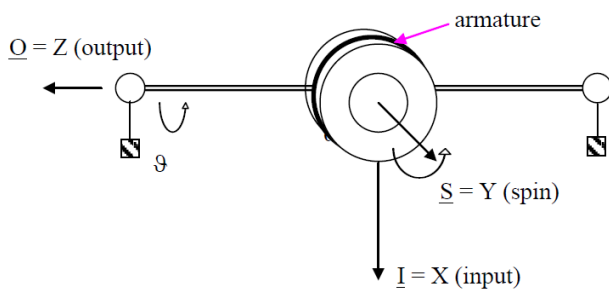


Figure 18: Gyro [17]

The rotor rotates around the \mathbf{S} axis and the support mechanism spins around the axis \mathbf{O} . The Euler equation of the system are:

$$\begin{cases} \omega_y J_z \dot{\theta} - \underbrace{I_R}_{rotor} \omega_R (\omega_z + \dot{\theta}) = M_x \\ I_R \dot{\omega}_R - \omega_x J_z \dot{\theta} = M_y \\ \underbrace{J_z}_{rot+arm+sup} \ddot{\theta} + I_R \omega_R \omega_x = M_z \end{cases} \quad (30)$$

The first 2 equations provide the reaction forces and the third one the angular velocity ω_x

As a steady state solution ω_x has the following value:

$$M_z = -k\theta - c\dot{\theta} \implies \omega_x = -\frac{k\bar{\theta}}{I_R \omega_R} \quad (31)$$

Simple Gyro noise modeling:

Every kind of measure is affected by noise , and the gyro copes with this issue as well:

$$\boldsymbol{\omega}_i^m = \boldsymbol{\omega}_i + \mathbf{n} + \mathbf{b} \quad (32)$$

with:

$$\mathbf{n} = \sigma_n \zeta_{\mathbf{n}} \quad (33) \qquad \qquad \dot{\mathbf{b}} = \sigma_b \zeta_{\mathbf{b}} \quad (34)$$

$\sigma_n \zeta_{\mathbf{n}}$ and $\sigma_b \zeta_{\mathbf{b}}$ are defined as white Gaussian noise with zero mean value and respectively standard deviation σ_n and σ_b .The source of noise for the first one,known as angular random walk (ARW) , is strictly associated with thermo-mechanical noise.Concerning the second one, called RRW (rate random walk), is related to the electric noise.To have the total noise contribution the 34 is integrated over time in all 3 components and summed with the 33.

6.2.8 Magnetometer:

A magnetometer is an instrument that measures the direction and strength of the magnetic field in the body frame. This device is operated for the attitude determination by knowing at the same time b_B and b_N , the local magnetic field and the inertial one. It is usually coupled with a Sun or an Earth horizon sensor, but not in this project. The output $\mathbf{A}_{B/N}^*$ is :

$$\mathbf{A}_{B/N}^* = \mathbf{A}_{eps} \mathbf{A}_{B/N} \quad (35)$$

\mathbf{A}_{eps} is the error matrix and $\mathbf{A}_{B/N}$ the ideal attitude:

$$\mathbf{A}_{eps} = \begin{bmatrix} \cos(\epsilon)\cos(\epsilon) & \cos(\epsilon)\sin(\epsilon)\sin(\epsilon) + \sin(\epsilon)\cos(\epsilon) & -\cos(\epsilon)\sin(\epsilon)\cos(\epsilon) + \sin(\epsilon)\sin(\epsilon) \\ -\sin(\epsilon)\cos(\epsilon) & -\sin(\epsilon)\sin(\epsilon)\sin(\epsilon) + \cos(\epsilon)\cos(\epsilon) & \sin(\epsilon)\sin(\epsilon)\cos(\epsilon) + \cos(\epsilon)\sin(\epsilon) \\ \sin(\epsilon) & -\cos(\epsilon)\sin(\epsilon) & \cos(\epsilon)\cos(\epsilon) \end{bmatrix} \quad (36)$$

In a similar manner , as seen with the gyroscope , it exists a model for the noise contribution.

$$\epsilon = p_{acc}\zeta_m \quad (37)$$

6.2.9 Magneto torquer:

A magnetic torquer is a satellite system for attitude control, detumbling, and stabilization built from electromagnetic coils. The magnetotorquer creates a magnetic dipole that interfaces with an ambient magnetic field, usually Earth's, so that the counter-forces produced provide useful torque.

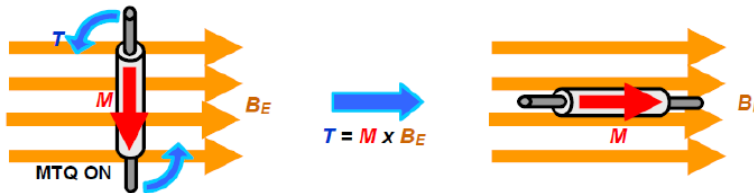


Figure 19: Magneto torquer in action [18]

The magnetic dipole \mathbf{m}_{MT} of the rods, is proportional to current i_{MT} flowing in it according to this relation:

$$\mathbf{m}_{MT} = c \mathbf{i}_{MT} \quad (38)$$

Next the torque is calculated:

$$\mathbf{t}_{mag} = \mathbf{m}_{MT} \times \mathbf{b}_b \quad (39)$$

Where \mathbf{b}_b is the Earth magnetic field vector in the body frame. Usually for de-tumbling there are three-orthogonal magnetic torquers for 3-axis control. However, it is a sort of underactuated system because one of the rods can be aligned with the magnetic field direction without producing torque. On the other hand, while de-tumbling, the spacecraft is rotating and as consequence the direction of the magnetic field changes.

The parameter to play with , while implementing a control law, is \mathbf{m}_{MT} . For the particular case under analysis see 7.1.3

6.2.10 Reaction wheels:

A reaction wheel is used primarily by spacecrafts for three axes attitude control, which doesn't require rockets or external applicators of torque. They provide a high pointing accuracy and are particularly useful when the spacecraft must be rotated by very small amounts, such as keeping a telescope pointed at a star.

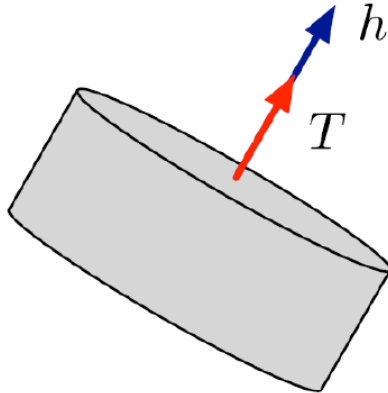


Figure 20: Reaction wheel model [19]

In particular \mathbf{A}^* is :

$$\mathbf{A}^* = \mathbf{A}^T (\mathbf{A} \mathbf{A}^T)^{-1} \quad (43)$$

6.2.11 Cold-Gas thrusters

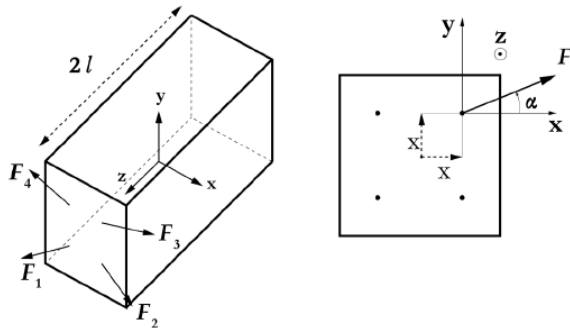


Figure 21: disposition of the thrusters [19]

Given the thruster configuration in the figure, it corresponds a torque matrix computed by taking the cross product between the force of each thruster and the moment arm:

$$\underline{\underline{T}}_1 = \begin{bmatrix} -x \\ -x \\ l \end{bmatrix} \times \begin{bmatrix} -F \cos \alpha \\ -F \sin \alpha \\ 0 \end{bmatrix} = \begin{bmatrix} lF \sin \alpha \\ -lF \cos \alpha \\ xF \sin \alpha - xF \cos \alpha \end{bmatrix}$$

The easiest way to provide a torque is to generate a set of forces not aligned with the center of mass. For Attitude control cold gas thrusters are very common and capable ,with few milli–Newton of applied force, to do the job.The key point is to switch them on and off on cue. They use a non reactive gas (He or N),stored at high pressure (approximately 30 MPa) .

The relative configuration matrix is :

$$\mathbf{T} = [\mathbf{T}_1 \quad \mathbf{T}_2 \quad \mathbf{T}_3 \quad \mathbf{T}_4] \quad (44)$$

In more detail:

$$T = \begin{bmatrix} IF \sin \alpha & IF \sin \alpha & -IF \sin \alpha & -IF \sin \alpha \\ -IF \cos \alpha & IF \cos \alpha & IF \cos \alpha & -IF \cos \alpha \\ xF \sin \alpha - xF \cos \alpha & xF \cos \alpha - xF \sin \alpha & xF \sin \alpha - xF \cos \alpha & xF \cos \alpha - xF \sin \alpha \end{bmatrix}$$

7 Control and determination Algorithms

7.1 De-tumbling

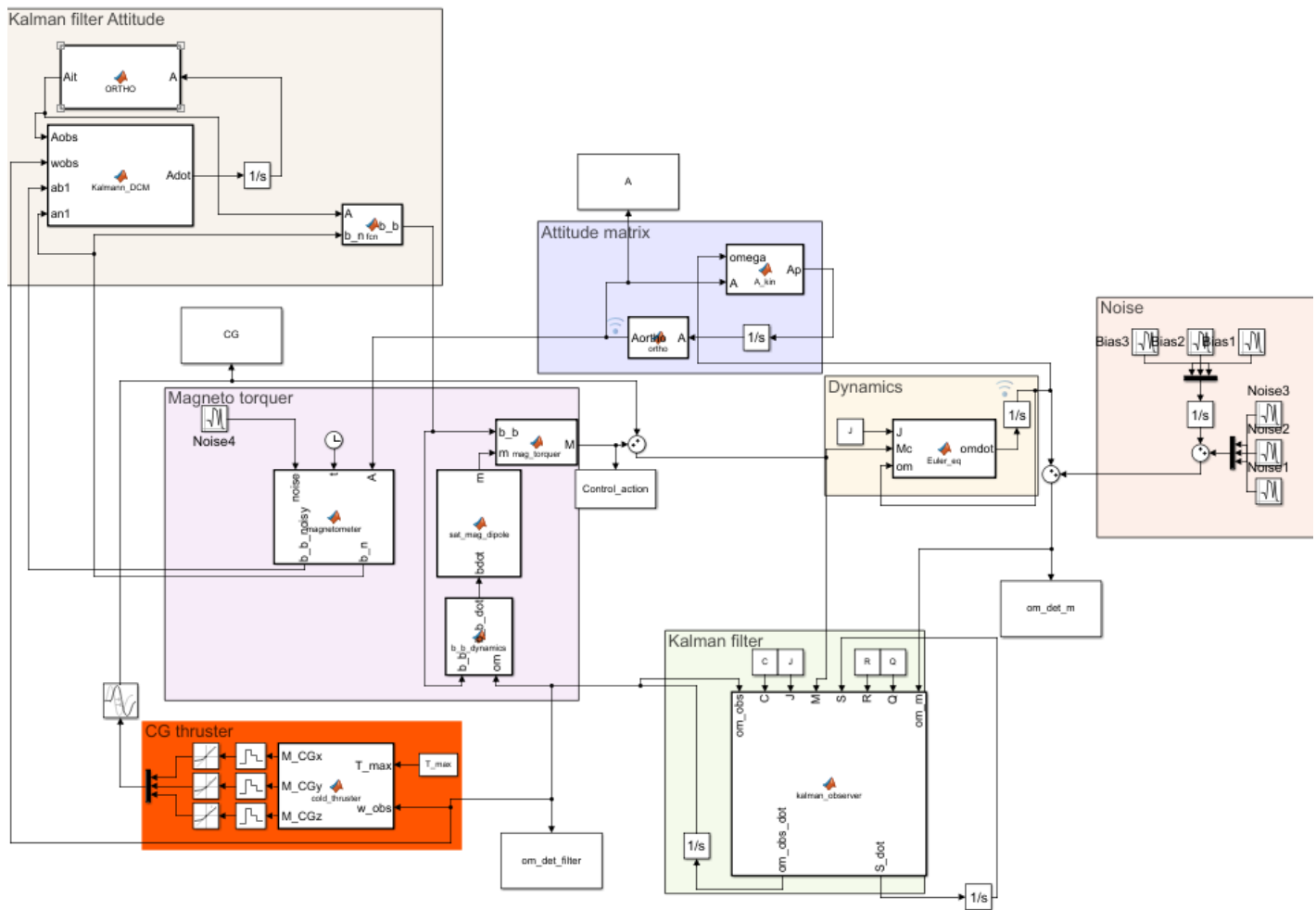


Figure 22: de-tumbling

7.1.1 Kalman Filter:

Kalman filtering is an algorithm that uses a series of measurements observed over time, containing statistical noise and other inaccuracies, and produces estimates of unknown variables that tend to be more accurate than those based on a single measurement alone. It is useful to reconstruct the states of an observable dynamic system:

Real system:

$$\begin{cases} \dot{\mathbf{x}} = \mathbf{f}(\mathbf{x}, \mathbf{u}) + \underbrace{\mathbf{w}}_{\text{disturbance}} \\ \underbrace{\mathbf{y}}_{\text{noisy signal}} = \mathbf{g}(\mathbf{x}, \mathbf{u}) + \underbrace{\mathbf{v}}_{\text{noise}} \end{cases} \quad (45)$$

reconstructed non linear system with noise filtering:

$$\begin{cases} \dot{\hat{\mathbf{x}}} = \mathbf{f}(\hat{\mathbf{x}}, \mathbf{u}) + \mathbf{L}(\mathbf{y} - \hat{\mathbf{y}}) \\ \underbrace{\hat{\mathbf{y}}}_{\text{filtered signal}} = \mathbf{g}(\hat{\mathbf{x}}) \end{cases} \quad (46)$$

In the assigned problem the reconstructed state is done by selecting \mathbf{C} as the identity matrix arbitrarily:

$$\begin{cases} \dot{\omega}_{x_{obs}} = \frac{I_y - I_z}{I_x} \omega_{y_{obs}} \omega_{z_{obs}} + l_{w_1} + \frac{M_x}{I_x} \\ \dot{\omega}_{y_{obs}} = \frac{I_z - I_x}{I_y} \omega_{z_{obs}} \omega_{x_{obs}} + l_{w_2} + \frac{M_y}{I_y} \\ \dot{\omega}_{z_{obs}} = \frac{I_x - I_y}{I_z} \omega_{x_{obs}} \omega_{y_{obs}} + l_{w_3} + \frac{M_z}{I_z} \end{cases} \quad \text{with } \mathbf{l}_w = \mathbf{L}(\boldsymbol{\omega} - \mathbf{C}\boldsymbol{\omega}_{obs}) \quad (47)$$

\mathbf{L} can be estimated through the solution of the following differential Riccati equation [20]:

$$\dot{\mathbf{P}} = \mathbf{P}\mathbf{A}^T + \mathbf{A}\mathbf{P} + \mathbf{Q} - \mathbf{P}\mathbf{C}^T\mathbf{R}^{-1}\mathbf{C}\mathbf{P} \quad (48)$$

$$\mathbf{L} = \mathbf{P}\mathbf{C}^T\mathbf{R}^{-1} \quad (49)$$

$$\mathbf{A} = \begin{bmatrix} 0 & K_x \omega_{z_{obs}} & K_x \omega_{y_{obs}} \\ K_y \omega_{z_{obs}} & 0 & K_y \omega_{x_{obs}} \\ K_z \omega_{y_{obs}} & K_z \omega_{x_{obs}} & 0 \end{bmatrix} = \frac{\partial \mathbf{f}}{\partial \boldsymbol{\omega}} \Big|_{\boldsymbol{\omega}_{obs}} \quad (50)$$

$$K_x = \frac{I_y - I_z}{I_x}, K_y = \frac{I_z - I_x}{I_y}, K_z = \frac{I_x - I_y}{I_z} \quad (51)$$

$$\mathbf{R} = \begin{bmatrix} \sigma_w^2 & 0 & 0 \\ 0 & \sigma_w^2 & 0 \\ 0 & 0 & \sigma_w^2 \end{bmatrix} \quad (52)$$

$$\mathbf{Q} = \begin{bmatrix} \sigma_v^2 & 0 & 0 \\ 0 & \sigma_v^2 & 0 \\ 0 & 0 & \sigma_v^2 \end{bmatrix} \quad (53)$$

7.1.2 Kalman Filter for DCM

The attitude matrix is reconstructed in this way:

$$\dot{\hat{\mathbf{A}}}_{\mathbf{B}/\mathbf{N}} = -[(\boldsymbol{\omega} + \boldsymbol{\alpha})^\wedge] \hat{\mathbf{A}}_{\mathbf{B}/\mathbf{N}} \quad (54)$$

Where :

$$\boldsymbol{\alpha} = k_{DCM}(\mathbf{a}_b \times \hat{\mathbf{A}}_{\mathbf{B}/\mathbf{N}} \mathbf{a}_n) \quad (55)$$

The reconstruction of the state by means of the Kalman filter (*as with the one for the dynamics*) is suitable for noise attenuation caused by the sensor measurement.

7.1.3 Control law for the Magneto Torquer:

From the theory a simple control law is derived for the magnetic torquers:

$$\mathbf{m} = -m_{max} \operatorname{sign}(\dot{\mathbf{b}}_b) \quad \text{with 1 magnetic torquer} \quad \mathbf{m} = -[m_{max} \operatorname{sign}(\dot{\mathbf{b}}_{b1}) \quad 0 \quad 0]^T \quad (56)$$

For a detumbling spacecraft \dot{b}_b is

$$\dot{\mathbf{b}}_b = -[\boldsymbol{\omega}]^\wedge \mathbf{b}_b \quad (57)$$

7.1.4 Bang Bang Control:

Knowing the thruster configuration, it can be calculated the maximum torque delivered in each axis T_{max_i} . For example :

$$|T_{max_i}| = 2lF \sin(\alpha) \quad (58)$$

As a consequence the maximum torque matrix is:

$$\mathbf{T}_{\max} = \begin{bmatrix} |T_{max_1}| & 0 & 0 \\ 0 & |T_{max_2}| & 0 \\ 0 & 0 & |T_{max_3}| \end{bmatrix} \quad (59)$$

The Bang-Bang control requires the following definition:

$$\mathbf{u} = -\mathbf{T}_{\max} \text{sign}(\boldsymbol{\omega}) \quad (60)$$

This formula is valid on with 12 or more thrusters , with only 4 thruster it is impossible to have the maximum torque simultaneously on the three axes. As matter of fact a suboptimal solution is found. A logic could be to activate the thrusters , which operate on the axis with the largest angular velocity.

For example :

$$\omega_{max} = \omega_x \implies \mathbf{u} = - \begin{bmatrix} |T_{max_1}| & 0 & 0 \\ 0 & 0 & 0 \\ 0 & 0 & 0 \end{bmatrix} \text{sign}(\boldsymbol{\omega}) \quad (61)$$

Also possible rise ,fall times , MIB and delays of the actuator are taken into account by using the blocks in **Simulink Rate Limiter** , **zero order hold** and **transport delay** . To avoid chattering the actuation should be switched off when:

$$|\omega_{max}| < \epsilon_{Cold-Gas} \quad (62)$$

7.2 Slew Manoeuvre:

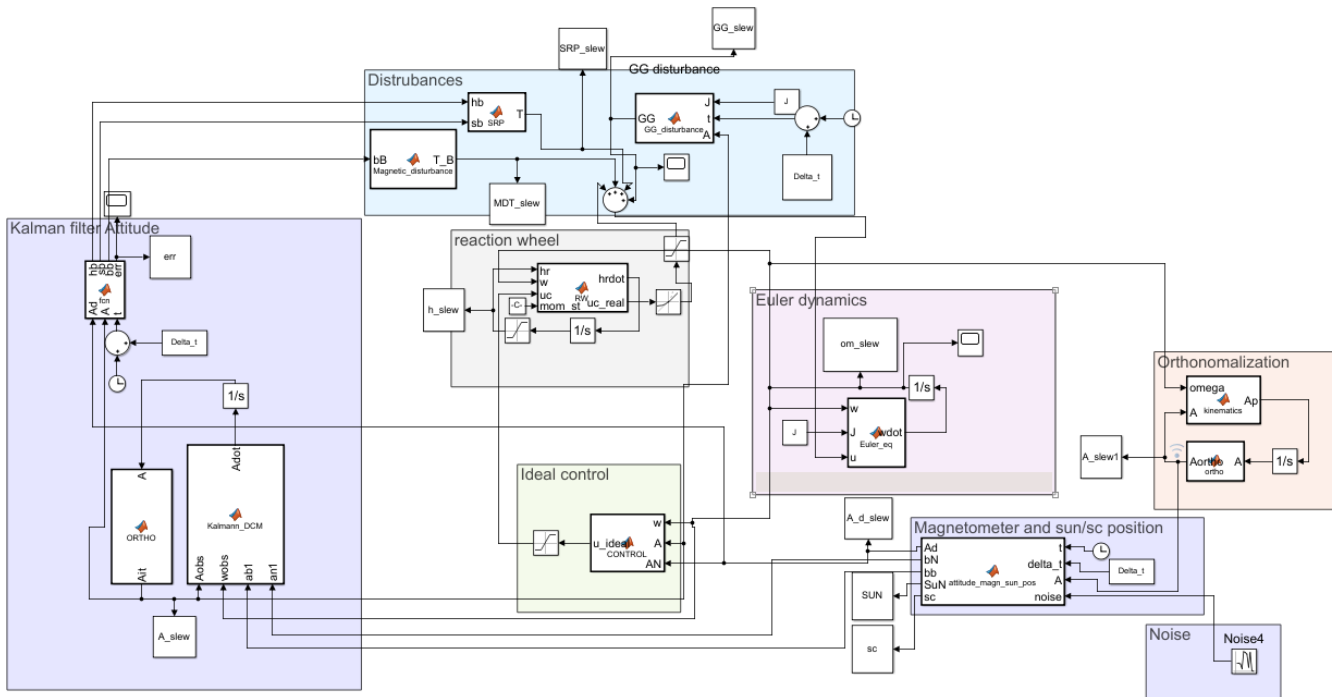


Figure 23: Slew Manoeuvre

7.2.1 Sun Pointing:

The main goal of the Cubesat is to rotate along its axis for an alignment with the Sun, that as first approximation has a fixed position in the space during the slew manoeuvre. Therefore to satisfy this requirement a desired attitude matrix \mathbf{A}_d is built in this way at $t^* = T_{det}$:

$$\mathbf{r}_{sc} = r_{sc} [\cos(n_e t) \quad \sin(n_e t) \quad 0] \quad (63)$$

$$\mathbf{r}_{sun} = r_{sun} [\cos(n_{sun} t + B) \quad \sin(n_{sun} t + B) \cos(23.45) \quad \sin(n_{sun} t + B) \sin(23.45)] \quad (64)$$

$$\mathbf{x}_1 = \frac{\mathbf{r}_{sun}(t^*) - \mathbf{r}_{sc}(t^*)}{\|\mathbf{r}_{sun}(t^*) - \mathbf{r}_{sc}(t^*)\|} \quad (65)$$

$$\mathbf{x}_2 = \frac{\mathbf{x}_3 \times \mathbf{x}_1}{\|\mathbf{x}_3 \times \mathbf{x}_1\|} \quad (67)$$

$$\mathbf{x}_3 = \frac{(\mathbf{r}_{sun}(t^*) - \mathbf{r}_{sc}(t^*)) \times (\mathbf{v}_{sun}(t^*) - \mathbf{v}_{sc}(t^*))}{\|(\mathbf{r}_{sun}(t^*) - \mathbf{r}_{sc}(t^*)) \times (\mathbf{v}_{sun}(t^*) - \mathbf{v}_{sc}(t^*))\|} \quad (66)$$

$$\mathbf{A}_d = \begin{bmatrix} \mathbf{x}_1 \\ \mathbf{x}_2 \\ \mathbf{x}_3 \end{bmatrix} \quad (68)$$

\mathbf{x}_1 is chosen as pointing axis because related to the direction with the maximum inertia, good for stability purposes. The quantification of the error between the desired attitude and the real one can be determined estimated as

$$err = trace(\mathbf{I} - \mathbf{A}_{B/N} \mathbf{A}_d^T) \quad (69)$$

7.2.2 Ideal Control:

The ideal control tries to figure out which is the correct value of torque that the reaction wheels need to grant. The expression is :

$$\mathbf{u}_{c_{ideal}} = -k_1 \boldsymbol{\omega}_e - \mathbf{e} \quad (70)$$

$$\boldsymbol{\omega}_e = \boldsymbol{\omega} \quad (71)$$

$$\mathbf{A}_e = \mathbf{A}_{B/N} \mathbf{A}_d \quad (72)$$

$$\mathbf{e} = k_2 (\mathbf{A}_e^T - \mathbf{A}_e)^V \quad (73)$$

7.2.3 Real Control:

In conclusion the ideal control becomes an input for the reaction wheel dynamics:

$$\dot{\mathbf{h}}_r = -\mathbf{A}^* (\mathbf{u}_{c_{ideal}} + \boldsymbol{\omega} \times \mathbf{A} \mathbf{h}_r) \quad (74)$$

$$\mathbf{u}_{c_{real}} = -\boldsymbol{\omega} \times \mathbf{A} \mathbf{h}_r - \dot{\mathbf{A}} \mathbf{h}_r; \quad (75)$$

Bear in mind that as for the Cold-Gas thruster case, a **rate limiter** is set for the variation of the torque in time and a **limiter** for the maximum momentum storage. In case of saturation a de-saturation procedure for the reaction wheels is necessary. for example:

$$\dot{\mathbf{h}}_r = -T sign(\mathbf{h}_r) \quad (76)$$

A decreasing value in time of the angular momentum of the RW yields undesired torques on the satellite. As a consequence, the control torque required for attitude stabilization can no longer be generated by the wheels. To prevent this phenomenon, the momentum of the reaction wheels has to be rapidly unloaded by magnetic torquers and/or thrusters.

7.3 Tracking

The Simulink file is equal to the slew one apart from minor changes due to control actuation laws.

7.3.1 Pointing

The procedure is the same as seen in 7.2.1, with a difference: the time is no more fixed so \mathbf{A}_d will evolve over time.

7.3.2 Ideal control:

Here the control law, compared to the Slew case, is transformed in a more complicated formulation because in presence of a time variant attitude \mathbf{a} . In its more general formulation the relation is:

$$\mathbf{u}_{c_{\text{ideal}}} = -k_1 \boldsymbol{\omega}_e - k_2 (\mathbf{A}_e^T - \mathbf{A}_e)^V + \mathbf{J} \boldsymbol{\omega} \times \boldsymbol{\omega} + \mathbf{J}(\mathbf{A}_e \dot{\boldsymbol{\omega}}_d - [\boldsymbol{\omega}_e^\wedge] \mathbf{A}_e \boldsymbol{\omega}_d) \quad (77)$$

In the event that the frame evolves slowly in time, a reduced version is proposed:

$$\mathbf{u}_{c_{\text{ideal}}} = -k_1 \boldsymbol{\omega}_e - k_2 (\mathbf{A}_e^T - \mathbf{A}_e)^V + \mathbf{J} \boldsymbol{\omega} \times \boldsymbol{\omega} \quad (78)$$

Definition of the involved variable:

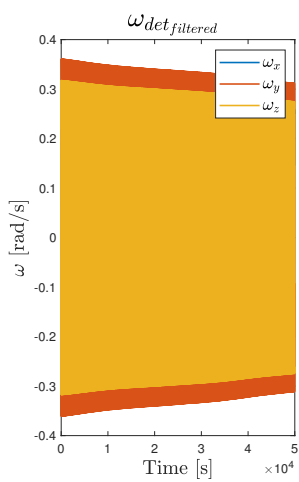
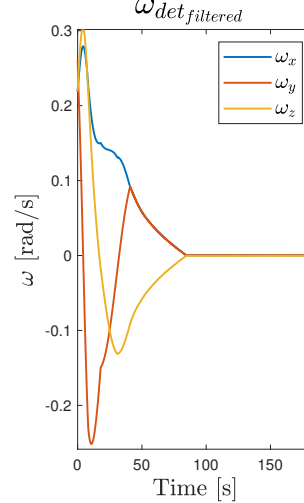
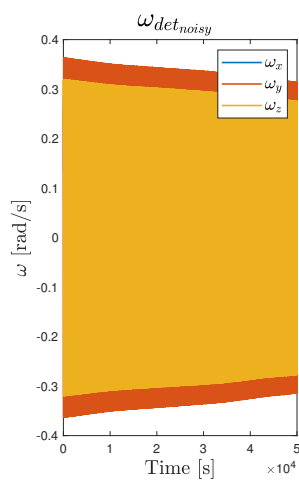
$$-\dot{\mathbf{A}}_d \mathbf{A}_d^T = [\boldsymbol{\omega}_d^\wedge] = \boldsymbol{\Omega} \quad (79) \qquad \qquad \mathbf{A}_e = \mathbf{A}_B / \mathbf{N} \mathbf{A}_d \quad (81)$$

$$\boldsymbol{\omega}_d = [-\boldsymbol{\Omega}(2,3) \quad \boldsymbol{\Omega}(1,3) \quad -\boldsymbol{\Omega}(1,2)]^T \quad (80) \qquad \qquad \boldsymbol{\omega}_e = \boldsymbol{\omega} - \mathbf{A}_e \boldsymbol{\omega}_d \quad (82)$$

The following passages for the real control are the same as 7.2.3

8 Results

8.1 Detumbling

Figure 24: $\omega_{detumbling}$ with only magneto torquersFigure 25: $\omega_{detumbling}$

In a GEO orbit the magnetic field of the Earth is so weak that the time required to de-tumble a 6U Cubesat is more than 50000 s, making the control actuation useless. This is the reason why Cold-Gas thrusters are introduced as part of the equipment. First of all the improvement thanks to the installation of 4 Cold-Gas thrusters is noticeable , compared to the previous solution , is able to bring to rest the satellite in less than 100 s. Secondly on the left hand side of 25 there is the reconstructed ω and on the right the one measured by the gyro. The Kalman filter combines the ability to follow the input signal with filtering high frequencing oscillation due to noise.

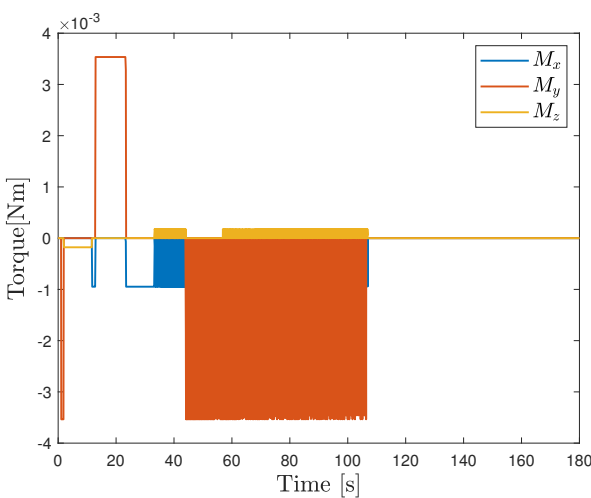


Figure 26: Cold-Gas thruster torque

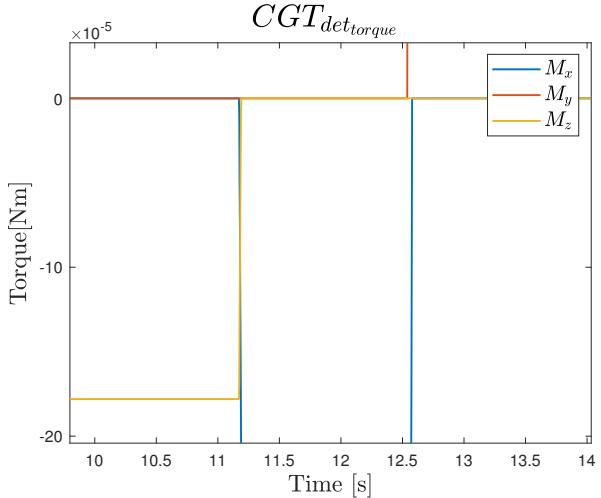


Figure 27: zoom of the Cold-Gas thruster torque

The 26 represents the evolution in time of the torque granted by the Cold-Gas thruster. From this figure it is understandable the functioning of the modified bang-bang control law. The torque is active on the different axes whenever the angular velocity is maximum. Between 40s to 100s, since the various components of ω

are almost equal in magnitude, there are a lot of firings. Furthermore after the de-tumbling the thrusters are not ignited any more in order to avoid chattering .The 27 is a zoom of the left hand side figure. Fall and rise time make not instantaneous the transition between on and off of as predicted by the real model .

8.2 Slew Manoeuvre

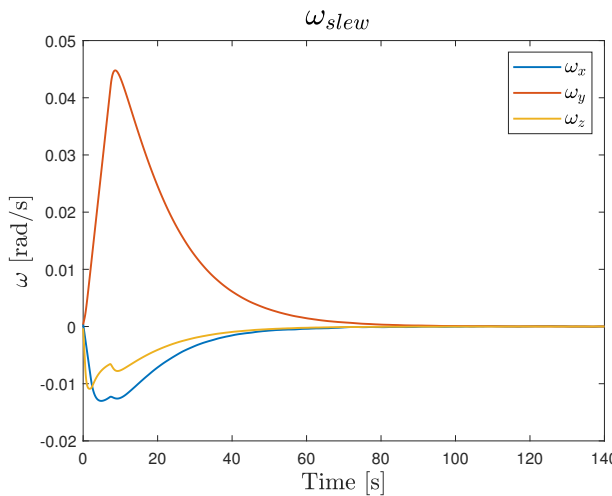


Figure 28: ω_{slew}

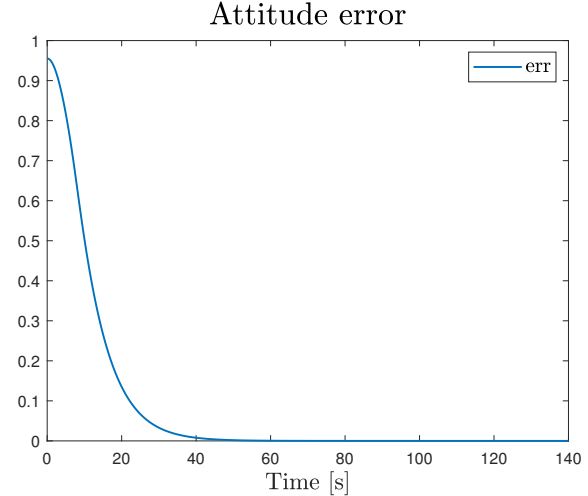


Figure 29: error

The goal of the Slew is to perform a rest to rest manoeuvre. It has to steer the axes according to the position of the Sun, which is assumed to be fixed in time in this short time frame. After a transient of 70– 80s it is capable of reaching the desired attitude. The formula used for 29 is explained in 7.2.2

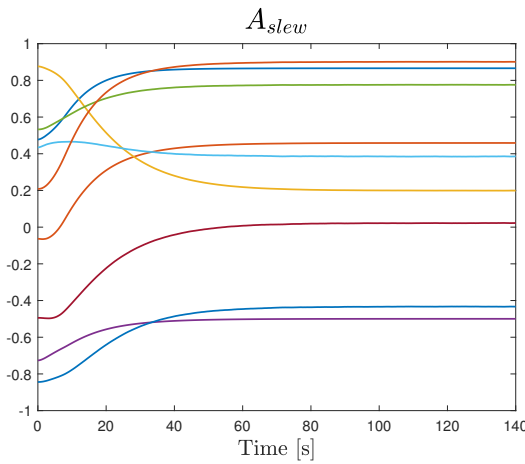


Figure 30: filtered attitude matrix

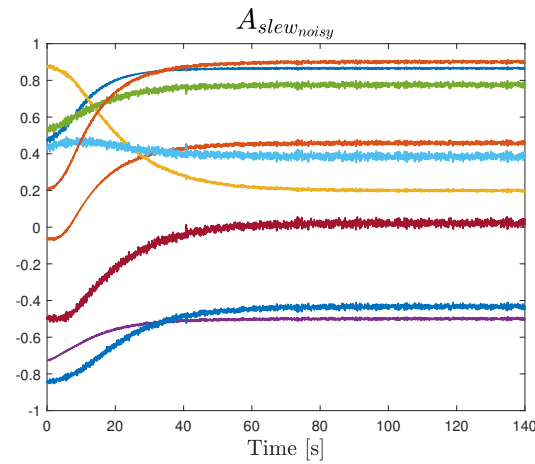


Figure 31: Noisy attitude matrix

The 30 and 31 show the importance of having a Kalman filter also for the attitude reconstruction. All the high frequency components associated to the magnetometer measurements are damped out through a suitable integral action. Similar results are derived in tracking.

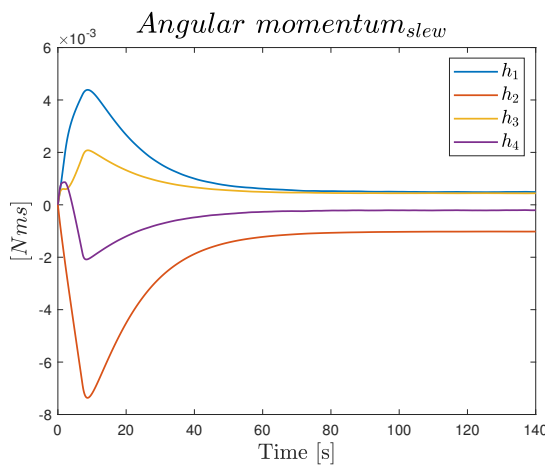


Figure 32: angular momentum for the 4 RW

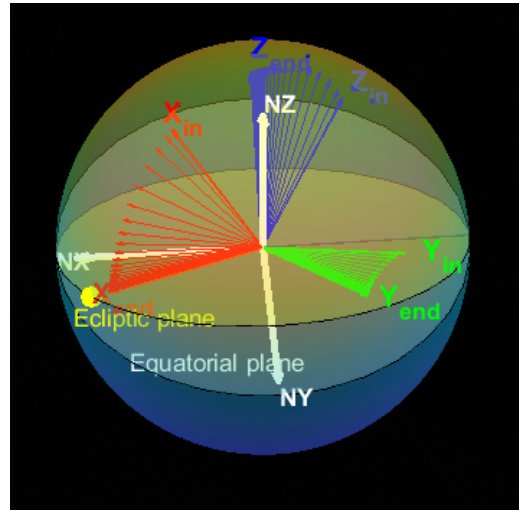


Figure 33: 3d motion

The 8.2 stands for the evolution in time of the angular momentum related to the 4 RW. None of them reach the saturation condition, but at the end there is a residual angular momentum. The 33 represents the evolution in time of the inertial principal axes during the slew manoeuvre. The yellow spot is the Sun position.

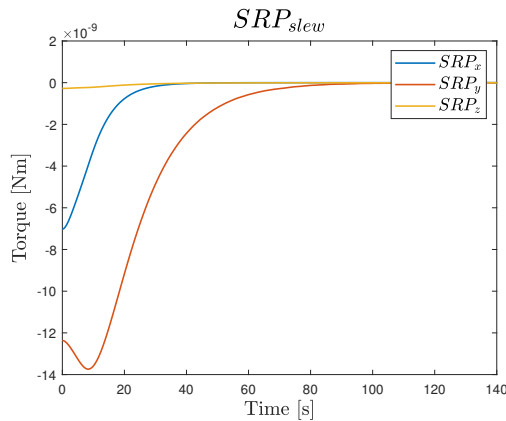


Figure 34: all the disturbances

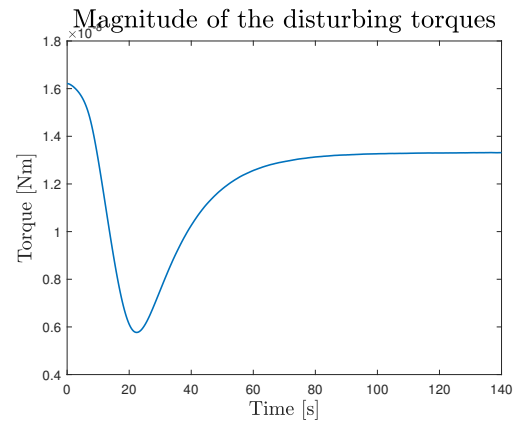
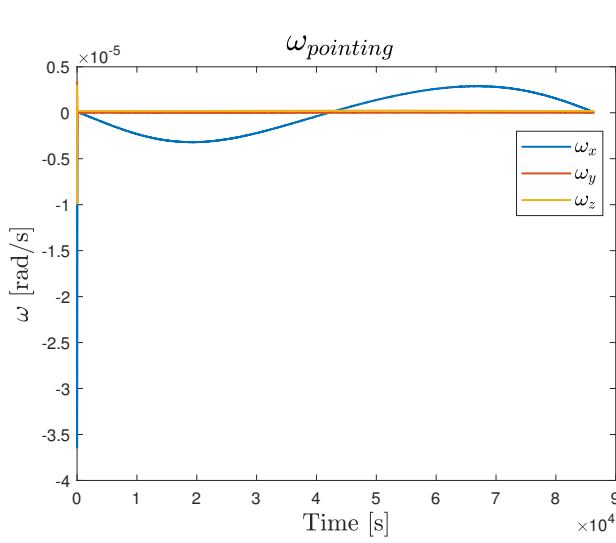
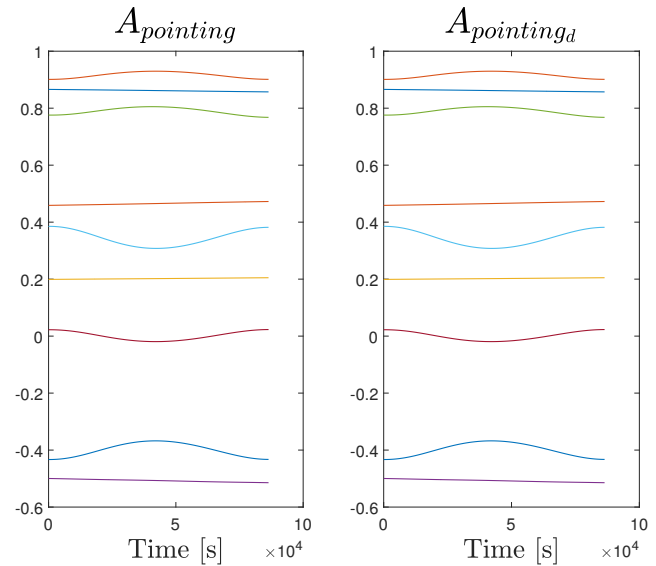


Figure 35: magnitude of the disturbances

A good indicator of the Slew manoeuvre is the SRP perturbation. Indeed if the spacecraft aligns its axes with respect to the sun, only the minimum amount of the outer surface will be illuminated, causing a small contribution of the disturbing torque. The total amount of the disturbances is of the order of 10^{-8} Nm and keeps the same order of magnitude also in tracking.

8.3 Sun Pointing

Figure 36: $\omega_{pointing}$ for 1 dayFigure 37: $A_{pointing}$ vs $A_{desired}$ for 1 day

Firstly the pointing part is simulated for one day and there are few features to point out:

1. The spacecraft is almost in a rest configuration because the rate of change of the \mathbf{A} matrix of the order of 1 day.
2. In addition both \mathbf{A} and \mathbf{A}_d have a period of one day. This can be explained recalling that the orbit is a GEO with 24 H of revolution period . The position of the Sun changes a little bit due to the relative motion.

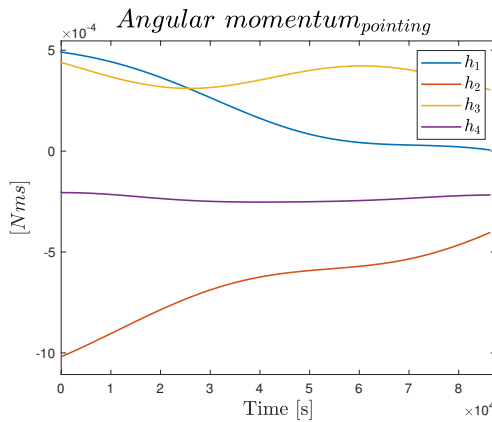
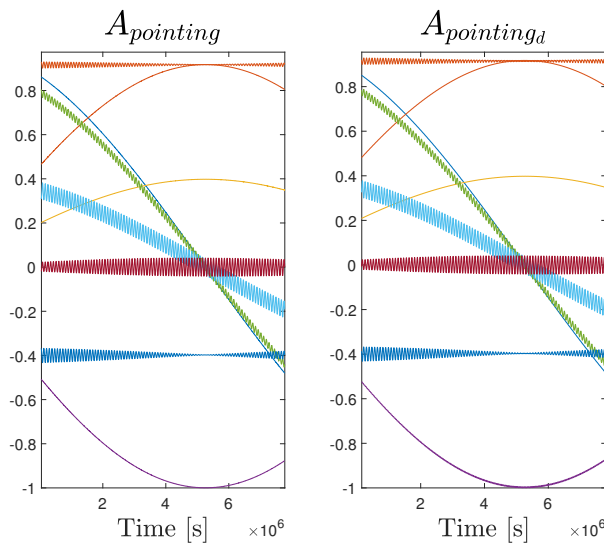
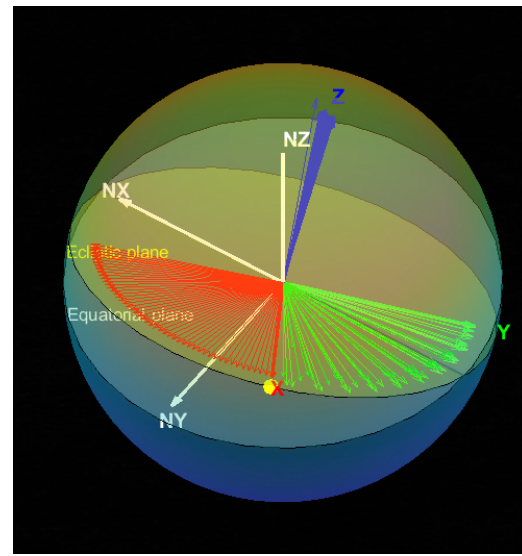


Figure 38: angular momentum for 1 day

Not only does not the slew require the de-saturation of the reaction wheels, but also the pointing. Remember that the maximum angular momentum is set to 10 [mNs]. There are not strong variation in time of the 4 components, because the manoeuvre requires small rotations in 1 day.

Figure 39: $A_{pointing}$ vs $A_{desired}$ for 90 daysFigure 40: 3_d motion

Secondly the system is integrated for 90 days and it is important underline this aspect: it is possible to notice 2 vibration modes, the former ,at a high frequency, is brought on by the motion of satellite with respect to the Earth. The latter, at lower frequency, instead is generated by the relative motion of the Sun in the inertial frame. The 40 is the evolution in time of the principal inertial axes in time during tracking.

9 Conclusions

Even if a lot of reasonable assumption are made in this project, the steps may be depicted for the work flow of Cubesat mission. The key point is to merge the requirements of the mission, the equipment available on the market, develop a consistent mathematical a physical model and tune the parameters in a acceptable range trying to get the desired results. Concerning the the output of the Simulink file 8 The control and the actuation is robust against both uncertainties of the measurements and outer disturbances. Furthermore the system is always able to adapt itself to new requested configurations in a short time.



References

- [1] Courtesy of https://www.nasa.gov/sites/default/files/atoms/files/nasa_csl_i_cubesat_101_508.pdf pp. 9-11 14
- [2] Courtesy of https://static1.squarespace.com/static/5418c831e4b0fa4ecac1bacd/t/5b75dfcd70a6adbee5908fd9/1534451664215/6U_CDS_2018-06-07_rev_1.0.pdf pp. 25
- [3] Courtesy of <https://www.sensonor.com/products/inertial-measurement-units/stim300/>
- [4] Courtesy of <https://www.cubesatshop.com/product/6-unit-cubesat-structure/>
- [5] Courtesy of <https://www.cubesatshop.com/product/nss-magnetometer/>
- [6] Courtesy of <https://www.cubesatshop.com/product/nctr-m012-magnetorquer-rod/>
- [7] Courtesy of <https://www.cubesatshop.com/product/cubewheel-medium/>
- [8] Biggs,D.J.,*Lab 9 slew motions with CMG and RW*, Course of Spacecraft attitude Dynamics And Control, pp 5, 2018
- [9] Courtesy of <https://www.cubesat-propulsion.com/wp-content/uploads/2015/10/Hybrid-adn-delta-5.pdf>
- [10] Courtesy of :https://www.researchgate.net/figure/Orbital-perturbations-as-a-function-of-altitude-fig6_323245224
- [11] Courtesy of :<https://www.slideshare.net/zuliana26/satellite-dynamic-and-control>
- [12] Courtesy of :<https://slideplayer.com/slide/9159756/>
- [13] Biggs,D.J.,*Supplementary notes of week 3*, Course of Spacecraft attitude Dynamics And Control, pp 2, 2018
- [14] Courtesy of :https://www.researchgate.net/figure/Schematic-of-the-effect-of-the-gravity-gradient-fig11_288917865
- [15] Biggs,D.J.,*Supplementary notes of week 6*, Course of Spacecraft attitude Dynamics And Control, pp 4, 2018
- [16] Biggs,D.J.,*Supplementary notes of week 7*, Course of Spacecraft attitude Dynamics And Control, pp 3, 2018
- [17] Biggs,D.J.,*Supplementary notes of week 8*, Course of Spacecraft attitude Dynamics And Control, pp 1, 2018
- [18] Biggs,D.J.,*Supplementary notes of week 10*, Course of Spacecraft attitude Dynamics And Control, pp 1, 2018
- [19] Biggs,D.J.,*Supplementary notes of week 9*, Course of Spacecraft attitude Dynamics And Control, pp 12, 2018
- [20] Courtesy of: http://cdn.intechopen.com/pdfs/39345/intech-optimal_solution_to_matrix_riccati_equation_for_kalman_filter_implementation.pdf